Effects of Al-Ti-B-RE + Al-10Sr master alloys on refinement and modification performances of A356 alloy

Liu Guanglei, Ding Ran, Guan Yunpeng, Yang Shanxin, Li Qinglong, Wang Huan

School of Materials Science and Engineering, Jiangsu University, Zhenjiang 212013, China

Liu Guanglei, 106409480@qq.com

Abstract. In this study, the Al-Ti-B-RE and Al-10Sr master alloy addition effects on refinement and modification performances of A356 alloys were investigated. The results demonstrated that the refinement and modification performances of the master alloy reduced along with the remelting times and the heat preservation duration increased. Following the fifth remelting, the A356 grain size was 130 μm, the secondary dendrite spacing was 13.4 μm, the tensile strength was 158 MPa, the elongation was 4.3 % and the brinell hardness was 70 HB. The mechanical performance decreased significantly compared to that of the A356 alloy without remelting. The heat preservation duration had a less significant effect on the A356 alloy properties than that of the remelting times. The secondary phase growth included the $AlTi_3$, TiB_2 and $Ti_2Al_{20}Re$ phases in the Al-5Ti-B-RE master alloy. In addition, the Sr adsorption quantity was declined on the Si phase surface. These were the two main reasons for the degradation of the refinement and modification performances of A356 alloys.

1. Introduction

The A356 is a common aluminum alloy utilized in aerospace, transportation and engineering industries due to its excellent casting properties, good corrosion resistance, net formability and machining performance. To expand the A356 alloy applications in high-end fields, researchers have focused on the grain refinement and Si metamorphic materials in some recent studies[1-2].

Currently, three methods of good refinement effect acquisition exist[3-5]: (1) The increase of the cooling speed during solidification; (2) Chemical methods, such as the use of a refining agent and modifier additions; (3) Physical methods, such as mechanical vibration, electromagnetic stirring and ultrasonic treatment. Among these methods, the grain refiner addition has become a hot research topic, due to the corresponding unique advantages, including a simple operation and no additional equipment. Na, K and other reagents have been gradually replaced by Al-Ti-B, Al-Sr, Al-RE, Al-Ti-C and composite refining agents[6-8], due to severe pollution and high corrosion issues. The Al-Ti-B master alloy is the most widely utilized refiner in China and abroad, with both $AlTi_3$ and TiB_2 particles in the main composition. Besides, the TiB_2 particles are extremely easy to segregate and precipitate, which lead in the remarkable inhibition of the refinement effect. In addition, the Al-Ti-B refiner is easy to lose its effectiveness, when the A356 alloy contains elements such as Zr and Cr[9-11]. Therefore, it is a proven necessity to research for new environmental protection requirements and a long-term stable grain refiner.

In recent years, a high number of colleges and universities, scientific research institutes at China and abroad have researched the rare earth additions in the refinement and the metamorphic ability

improvement of Al-Ti-B alloys. Although the research content mainly includes the addition of the Al-Ti-B-RE alloy, as a rare earth recipe, the preparation and the addition of a refining agent[12-14], research on A356 alloy regarding modification and refinement performance and long residual action by the addition of Al-Ti-B-RE or Al-10Sr master alloys is non-existent. Based on this, The modification and refinement performance along with the long residual action of Al-5Ti-1B-1Re and Al-10Sr master alloys were observed and discussed from multiple perspectives. These include mechanical properties, microstructure, grain size, secondary dendrite arm spacing, master alloy microstructure and electron probe scanning. Also, the corresponding affecting laws obtained from this study would provide the theoretical and experimental basis for the environmental conservation and the long-term stability control over the performance and grain refinement effect of the A356 alloys.

2. Experimental Procedure

2.1. Al-5Ti-1B-1Re master alloy preparation

The dry potassium fluoroborate powders and the dry potassium fluotitanate powders were mixed according to the Ti:B mass ratio of 5:1. These powers along with pure aluminum powders were subsequently ball milled in a ball grinder (50 r/min) for 10h and cold pressed compactly by a universal testing tensile machine. The industrial pure aluminum was melt in a well type resistance furnace at 760 ℃. The cold-pressed compacted and enriched with Ce rare earth (chemical composition: Ce: 58.5 wt%; La: 35.9 wt%; else: 5.6 wt%) samples were wrapped in an aluminum foil and added into molten aluminum. To ensure the complete dissolution the cold-pressed compacted and rich cerium rare earths into molten aluminum, the heat preservation lasted a certain amount of time. Consequently, the temperature was adjusted to 825 ℃. In parallel, the melts were stirred thoroughly by a graphite stirring bar for 5 mins. Moreover, the melts were retained still for 30mins. Following the refinement and degassing treatment at (780±5) ℃, the melts were poured into an iron mold to obtain the Al-5Ti-1B-1Re ingot.

2.2. Refining capacity and long-term experiments

The A356 alloy ingot was utilized as the matrix material (chemical composition presented in Table 1), whereas both Al-5Ti-1B-1Re and Al-10Sr master alloys were utilized as additives (chemical composition presented in Table 2). The pit type furnace was utilized for melting. The graphite crucible was preheated firstly at 500 ℃ for 30 mins, and the first melting process was conducted at 760 ℃. When the A356 alloy was completely melt, the temperature was adjusted to 800 ℃. Then, the 0.8 wt% Al-5Ti-1B-1Re and 0.3 wt% Al-10Sr master alloys were added into the molten alloy for the remelting treatment with a slight stirring by the graphite rod. Following, the temperature was adjusted to 720 ℃ and the melt was stirred once every 5 mins during the 20 mins. Subsequently to the last stir, the melts sustained a heat preservation for 5 mins. A 0.5 wt% HGJ-2 aluminum alloy sodium free refining agent was then added into the melts. Subsequently, the melts sustained heat preservation for another 5 mins. Lastly, the degassing process was executed and the melts were poured into a metal mould.

Table 1 Chemical composition of A356 alloys (wt%)

Si	Mg	Cu	Ti	Mn	Zn	Fe	Al
6.5～7.5	0.2～0.4	≤0.2	≤0.2	≤0.1	≤0.1	≤0.2	Bal

Table 2 Chemical composition of Al-5Ti-1B-1Re and Al-10Sr alloys (wt%)

	Si	Cu	Mg	Fe	Ti	B	Sr	RE	Al
Al-5Ti-1B-1Re	0.11	—	—	0.05	5.05	1.01	—	1.03	Bal
Al-10Sr	0.105	—	—	0.09	—	—	10.06	—	Bal

The remelting process can be described as follows: the A356 alloys with the remelting treatment (following refinement and modification) were remelted for 1, 3, 5 or 7 times. The specific process parameters were: the temperature was 760 ℃ and the heat was preserved for 10 mins. A full stir was

executed during heat preservation. Refinement and degassing were conducted prior to the melts were poured into the standard tensile test bar metal mold. The shape and size of the test bar is presented in Figure 1. The heat preservation was: when the A356 alloy were completely melt, following the remelting treatment, the temperature was retained at 760 ℃ for 30 mins, 60 mins, 120 mins, 180 mins or 240 mins, respectively. The same operation was utilized for the sample preparation following various heat preservation durations. Finally, the T6 heat treatment of the samples following remelting and heat preservation processing was executed. The process parameters were: solution at 535 ℃ for 5 h, quenched in 70 ℃ hot water, natural aging for 2 h and artificial aging at 165 ℃ for 4 h. The final samples were prepared, demonstrating the modification and refinement performance along with the long residual action of the master alloys.

The tensile tests were executed on a universal tensile tester, the metallographic and brinell hardness test specimens were severed from both ends of the tensile test bar, following the tensile tests. The microstructures of the A356 and master alloys were assessed by a Leica optical microscope (OM) and a JMS-7001F scanning electron microscope (SEM). The grain size of the microstructure and the secondary dendrite spacing were measured by the Image-Pro Plus 6.0 software.

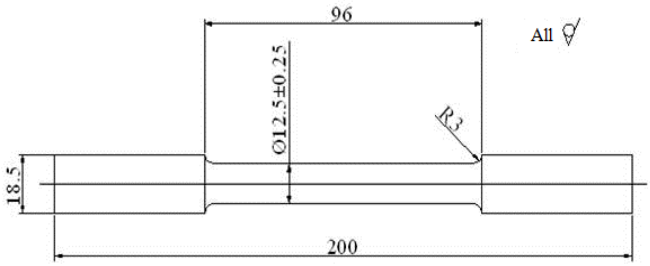

Fig.1 Tensile test bar dimensions

3. Results and Discussion

3.1. Remelting effects on A356 alloy properties and microstructure

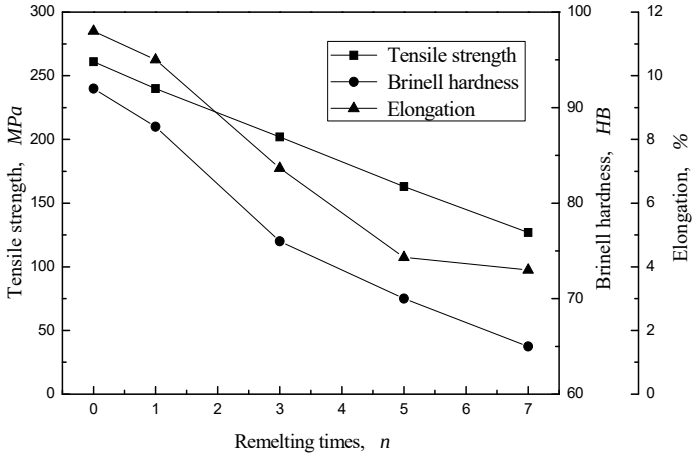

Fig.2 Mechanical properties of A356 (T6) alloys following remelting

The mechanical properties of the as-cast A356 alloy were poor. The tensile strength was 165 MPa, the elongation was 1.26 % and the brinell hardness was 61 HB. The mechanical properties of the A356 (T6) alloys with the remelting treatment were higher, as presented in Figure 2. The tensile strength was 261 MPa, the elongation was 11.4 % and the brinell hardness was 92 HB. Following the first

remelting, the mechanical properties remained satisfactory. The mechanical properties declined as the remelting number of times increased, as presented in Figure 2. Following the fifth remelting, the mechanical properties deteriorated, the tensile strength was 158 MPa, the elongation was 4.3% and the brinell hardness was 70 HB. Following the seventh remelting, the tensile strength was 127 MPa, the elongation was 3.9 % and the brinell hardness was 65 HB. Apparently, following the fifth remelting, the mechanical properties of the A356(T6) alloys were lower than those of the as-cast A356, Al-5Ti-1B-1RE and Al-10Sr master alloys, which no longer contributed to the modification refinement performance.

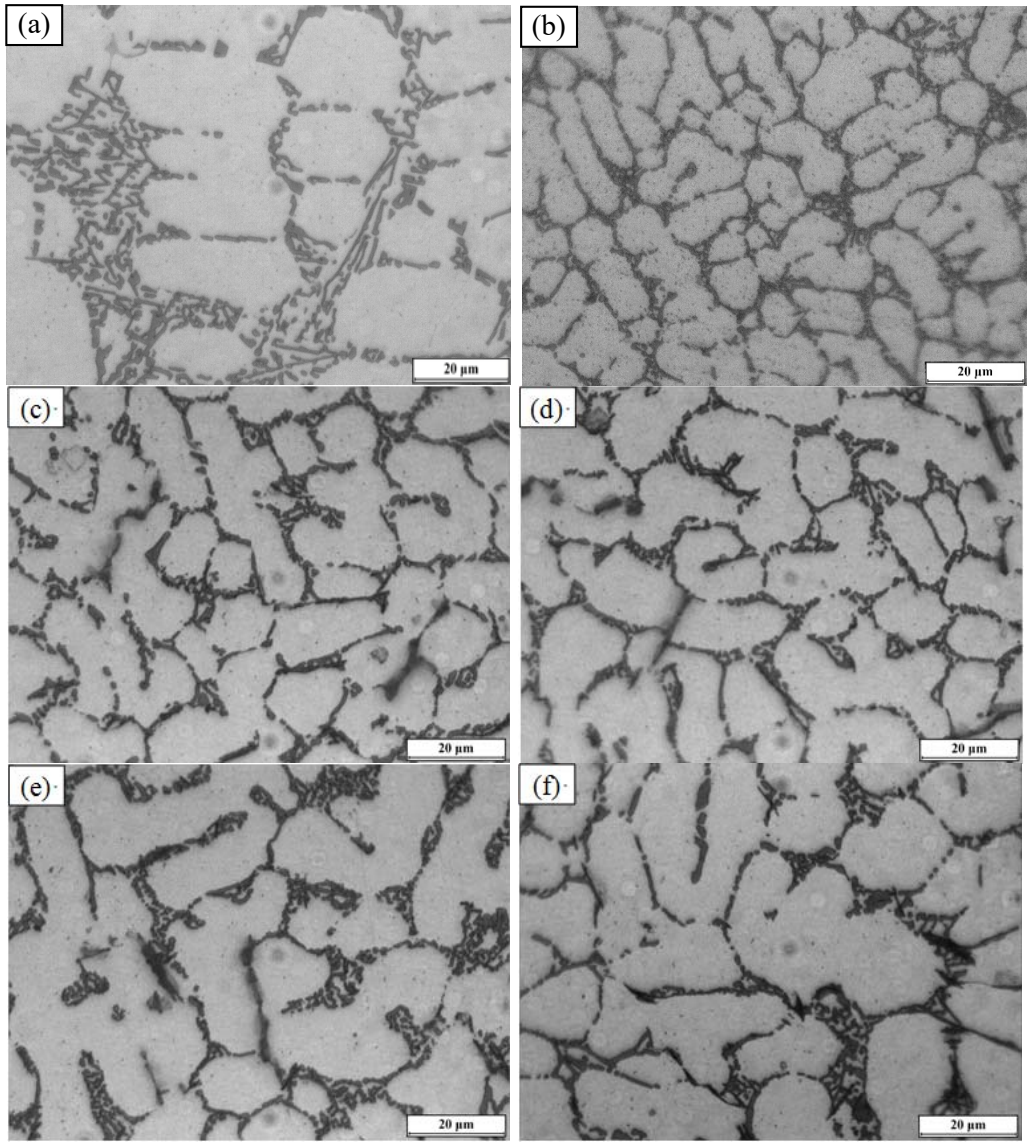

Fig.3 Microstructure of A356 (T6) alloy following remelting

(a) as-cast A356 alloy; (b) A356 (T6) alloy following remelting treatment;
(c) A356(T6) alloy following one remelting; (d) A356(T6) alloy following three remeltings;
(e) A356(T6) alloy following five remeltings; (f) A356(T6) alloy following seven remeltings

The effect of remelting on the A356 (T6) alloy on the melt-treatment microstructures are presented in Figure 3. It was demonstrated that: the primary α-Al phase in the as-cast A356 alloys was coarse; the growth shape followed the dendrites shape with a strong orientation. The eutectic Si shape was a coarse needle and disorderly distributed within the α-Al matrix, as presented in Figure 3(a). Following

remelting, the α-Al phase size was lower, the shape of most Si phases was granular and the short rod is presented in Figure 3(b). It was demonstrated that both Al-5Ti-1B-1RE and Al-10Sr master alloys contributed significantly to the refinement and phase transformations, which improved the mechanical properties of the A356 alloys. As the remelting times increased, the α-Al size was higher and grew in the form of dendrites. Although the Si phase size was also increased, its average shape became either acicular or of long strips, as presented in Figure 3(c~f).

3.2. Effects of heat preservation on the A356 alloy properties and microstructure

The effects of heat preservation on the properties of A356 (T6) alloys with the remelting treatment are presented in Table 3. It was demonstrated that: the heat preservation lasted 60 mins, the mechanical properties reached higher values, the tensile strength, the elongation and the brinell hardness were 246 MPa, 10.6%, 88 HB, respectively. As the heat preservation holding duration increased, the A356 (T6) alloy mechanical properties displayed a linear downward trend. When the heat preservation was 240 mins, the tensile strength was 220 MPa, the elongation was 8.5 % and the brinell hardness was 76 HB. Compared to the 60 mins holding duration, the tensile strength, the elongation and the brinell hardness were decreased by 10.5 %, 19.8 % and 13.6 %, respectively. In contrast, compared to the as-cast A356, the mechanical properties were similar, proving that the master alloy had an excellent long-term behaviour.

Table 3 Mechanical properties of A356(T6) alloys following heat preservation holding durations

Holding duration, min	Tensile strength, MPa	Elongation, %	Brinell hardness, HB
30	258	11.1	90
60	246	10.6	88
120	240	10.3	85
180	235	9.9	80
240	220	8.5	76

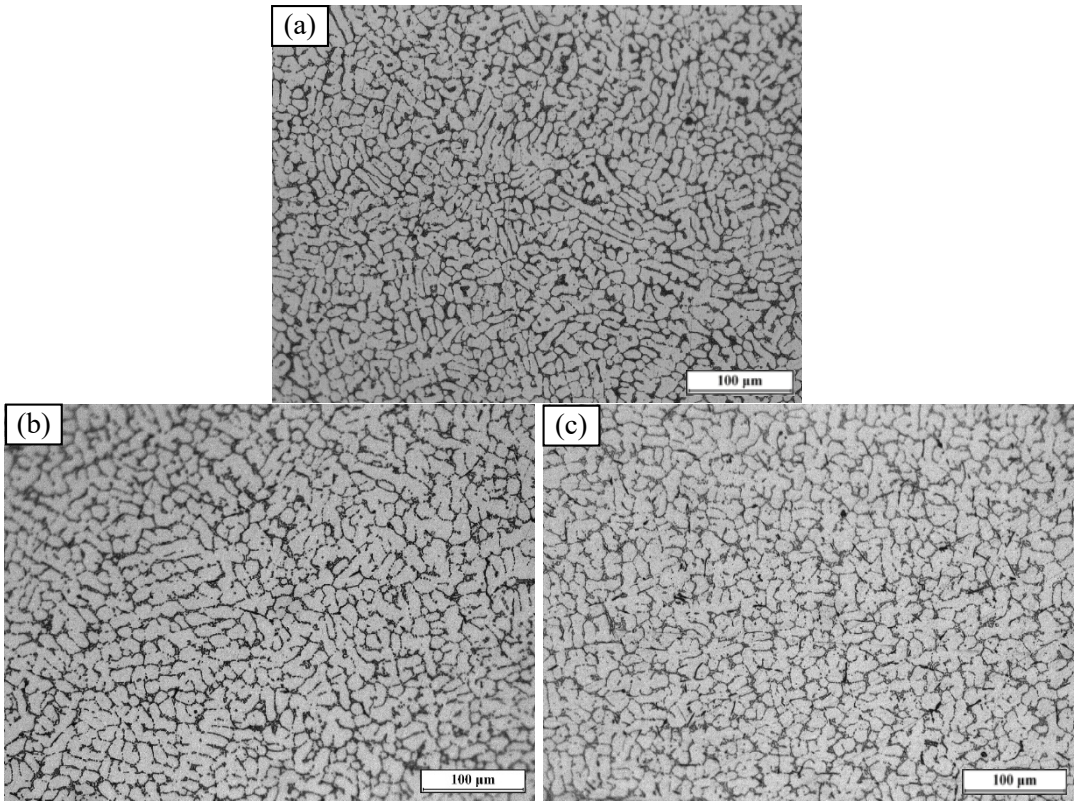

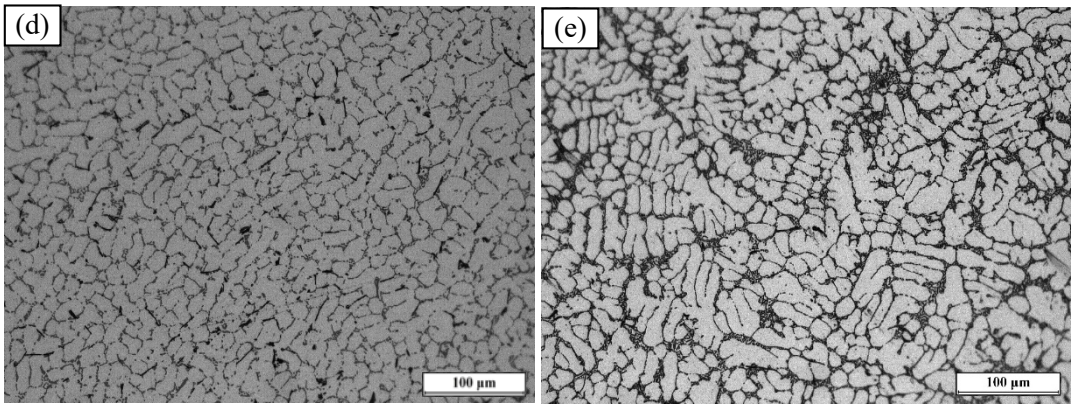

Fig.4 Microstructure of A356 (T6) alloys following various heat preservation holding durations (a)30 mins; (b)60 mins; (c)120 mins; (d)180 mins; (e)240 mins

The effects of heat preservation on the A356 (T6) alloy microstructure with melt-treatment are presented in Figure 4. As the heat preservation holding time increased, the white α-Al and dark Si phased increased, and the intergranular area branches also increased. However, the changes were not apparent and consequently the alloy mechanical properties were slightly deteriorated. Based on the aforementioned analysis, the remelting had a more significant effect on the mechanical properties and microstructure of A356 alloys than the heat preservation holding time and this conclusion had a key significance for the practical production.

3.3. Grain sizes and secondary dendrite spacing analysis

The grain sizes and the secondary dendrite arm spacing of the A356 (T6) alloys with the remelting treatment, the remelting and the heat preservation were measured by the Image Pro Plus 6.0 software, and the results are presented in Table 4. It could be observed that both the remelting and the heat preservation duration had adverse effects on both grain sizes and the secondary dendrite spacing, whereas the remelting times had a quite substantial effect.

Table 4 Grain size and secondary dendrite arm spacing of A356 (T6) alloys with remelting times and heat preservation processing

	remelting treatment A356(T6)	remelting processing, times				heat preservation processing, mins				
		1	3	5	7	30	60	120	180	240
grain size, μm	101	104	119	130	143	102	113	122	131	136
secondary dendrite arm spacing, μm	7.3	9.5	10.3	13.4	15.2	8.3	9.8	11.1	13.3	14.2

3.4. Master alloy refinement and modification performances analysis

The qualitative phase analysis of the Al-5Ti-1B-1Re is presented in Figure 5. The XRD diffraction results demonstrated that $TiAl_3$, TiB_2 and $Ti_2Al_{20}Re$ were the main secondary phase particles, which played the refining role in the grain refiner. In contrast, the secondary phase particles especially for $Ti_2Al_{20}Re$ and $TiAl_3$ phase, which had similar morphology, could not be distinguished in the figure. To execute the quantitative analysis 3 points were selected as electron probes in the microstructure of Al-5Ti-1B-1Re master alloys and the test results were as follows.

The mole ratio of each element is presented in Figures 6 (b) (c) (d). In contrast with the particle phase in Figure 6 (a), the white phase in point 1 was the AlTiRe phase, the corresponding chemical formula was $Ti_2Al_{20}Re$, the gray phase in point 2 was the $TiAl_3$ phase, the low-sized gray phase in

point 3 was the TiB_2. The Al-5Ti-1B-1Re change following remelting and heat preservation was apparent. According to the Ostwald coarsening mechanism[15], to release the rest of the interface energy, the higher-sized grain refiner would increase further, based on the dissolution of the lower-sized grain refiner particles, so that the number of intermetallic compound particles is reduced and the size is increased simultaneously during solidification[16]. As the remelting time and the heat preservation duration was increased, the secondary phase particles size was gradually increased from a tiny particle block to a coarser block, especially for both $AlTi_3$ and $Ti_2Al_{20}Re$. The TiB_2 particles began to segregate and formed as a tightly packed nest-like distribution, therefore the numbers of the effective nucleation core were apparently reduced. This was the reason for the A356 microstructure and mechanical properties deterioration as the remelting time and the heat preservation duration was increased.

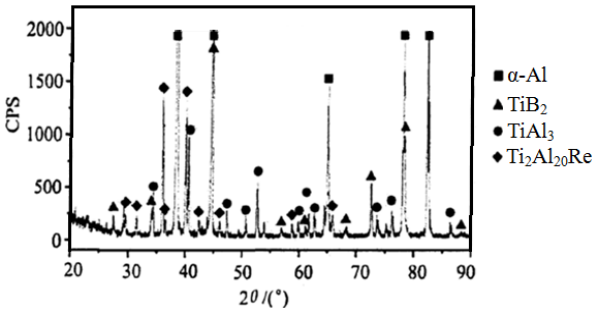

Fig.5 XRD pattern of Al-5Ti-1B-1Re master alloys

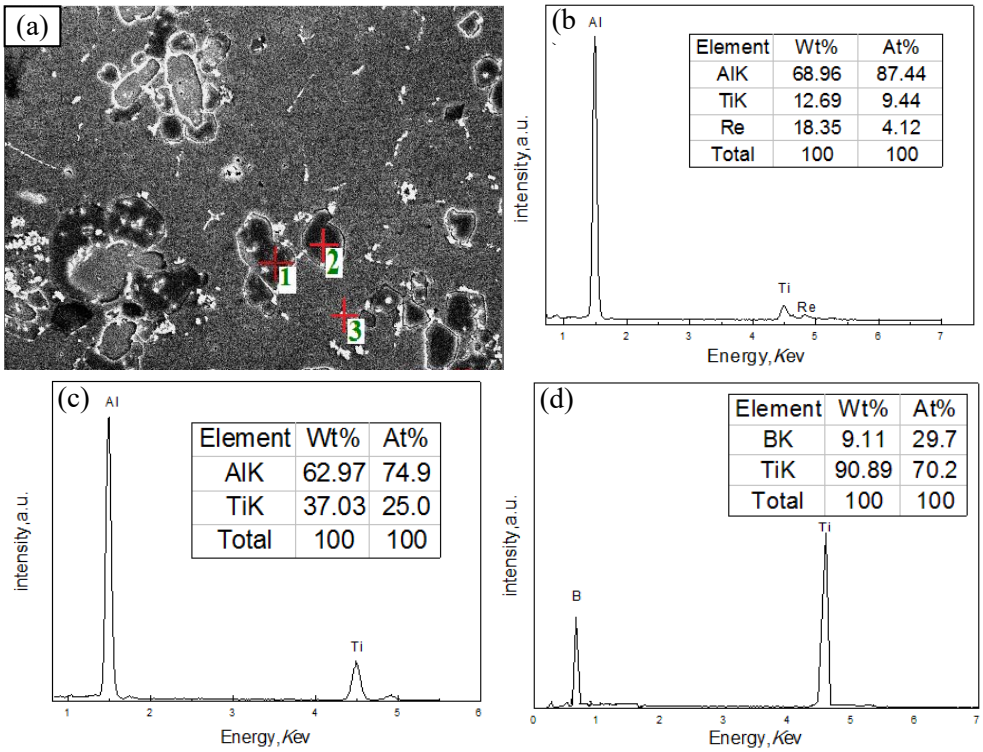

Fig.6 Spectra of Al-5Ti-1B-1Re quantitative analysis

(a) Al-5Ti-1B-1Re master alloy microstructure; (b) refiner Place 1 element content; (c) refiner Place 2 element content; (d) refiner Place 3 element content

The microstructure and EDS test results of the Al-10Sr master alloys and the modification effect are presented in Figures 7 and 8. It was demonstrated that the scanning point phase consisted of Al and Sr, whereas the atomic number ratio of Al / Sr was 4:1. Consequently, the chemical formula was the Al_4Sr. When the Sr in the Al_4Sr phase was converted to the free Sr, the Sr could contribute to phase transformations. Based on the literature[17], following the Al-Sr master alloy addition into the A356 melt, an incubation period for the Al_4Sr phase existed where the free Sr was isolated and only the Sr adsorption on the {111} Si could produce the metamorphism . Therefore, the eutectic Si embryos were formed; the embryos cumulatively grew into the critical crystal nucleus. Following, a higher number of tetrahedrons were absorbed into the nucleus to reduce the surface free energy. During growth, the metamorphic elements were adsorbed in the growth steps of Si, changed the Si formation from the step growth mechanism to the twin concave valley mechanism, and a high number of twin systems self-replication led the eutectic Si growth along the horizontal direction. The Sr absorption on the Si phase surface was physical being indifferent to the Si phase, the growth speed and was not sensitive to cooling speed, when the quality of Sr adsorption on the {111} Si crystal face reached a saturated value, finally producing a complete metamorphism[18]. Following effective metamorphism, the morphology of the eutectic Si phase became rounded and lower-sized, whereas the mechanical properties improved. The contrasting morphology of the Si phase prior to and following the metamorphism, as presented in Figure 3, fully proved the metamorphic effect existence of Sr on the Si phase.

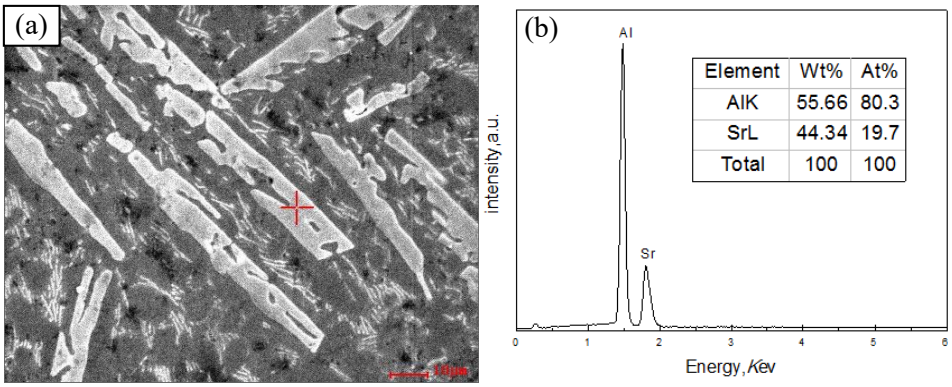

Fig.7 Spectrum of Al-10Sr quantitative analysis

(a) Al-10Sr master alloy microstructure; (b) refiner Point element content

As the remelting time and the heat preservation duration increased, the Sr should disappear due to oxidation reaction. When the quality of Sr decreased to a critical value, the Si phase would lose the metamorphic effect. In addition, the addition of Sr deteriorated the density of the A356 melt surface oxidation film and, thus, the integrity, whereas the protection effect of the oxide film was significantly reduced. This was the second main reason for the A356 alloy microstructure and mechanical properties deterioration as both the remelting time and the heat preservation duration was increased.

4. Conclusions

(1) Compared to the as-cast A356 alloys, the tensile strength, the brinell hardness and the elongation of the A356 with the addition of a 0.8 wt% of Al-5Ti-1B-1Re and a 0.3 wt% of Al-10Sr master alloys increased to 96 MPa, 31 HB and 10.14 % respectively.

(2) Both Al-5Ti-1B-1Re and Al-10Sr master alloys could result in an excellent refinement metamorphism and a long residual action on the A356 alloys. Following the fifth remelting and the heat preservation for 240 mins, the A356(T6) alloys that sustained the remelting treatment still displayed a good performance.

(3) Both remelting and heat preservation times had a certain deterioration degree on the mechanical properties, grain size and secondary dendrite spacing of the A356 alloys. The remelting had a significant effect.

(4) The secondary phase growth included the $AlTi_3$, TiB_2 and $Ti_2Al_{20}Re$ phases in the Al-5Ti-B-RE master alloy and the Sr adsorption quantity declined on the Si phase surface and these were the main reasons for the degradation of both the refinement performance and the long residual action of the A356 alloys.

Acknowledgements
This work was financially supported by the Technology Innovation Fund Project of High-tech Small and Medium Enterprises, the Science and Technology Department of Jiangsu Province (BC2012211), the Postdoctoral Research Funding Plan in Jiangsu Province (1601055C) and the Advanced Talent Research Fund of Jiangsu university (14JDG126).

References
[1] Aguirre-De la Torre E., Perez-Bustamante R., Camarillo-Cisneros J., Gomez-Esparza C.D., Medrano-Prieto H.M., Martinez-Sanchez R., Journal of Rare Earths. 31 (2013) 8, 811-816.
[2] Wang Tongmin, Zheng Yuanping, Chen Zongning, Zhao Yufei, Kang Huijun, Materials and design. 64 (2014) 185-193.
[3] Xu Cong, Xiao Wenlong, Zhao Weitao, Wang Wenhong, Hanada Shuji, Yamagata Hiroshi, Ma Chaoli, Journal of Rare Earths. 33 (2015) 5, 553-560.
[4] Jia Yandong, Cao Fuyang, Ma Pan, Liu Jingshun, Sun, Jianfei, Wang Gang, Journal of Iron and Steel Research, International. 23 (2016) 1, 14-18.
[5] Liu Mengxiang, Chen Jianmei, Advances in Material Science, Mechanical Engineering and Manufacturing. 744 (2013) 339-344.
[6] Wang Kui, Cui Chunxiang, Wang Qian, Zhao Lichen, Hu Yuan, Journal of Rare Earths. 31 (2013) 3, 313-318.
[7] Agne Matthias T., Anasori Babak, Barsoum Michel W., Journal of Phase Equilibria and Diffusion. 36 (2015) 2, 169-182.
[8] Birol Y., International Journal of Cast Metals Research. 26 (2013) 5, 283-288.
[9] Kumar G. S. Vinod, Murty B. S., Chakraborty M., Journal of Alloys and Compounds. 472 (2009) 1-2, 112-120.
[10] Huang Yuanchun, Xiao Zhengbing, Liu Yu, Journal of Central South University. 20 (2013) 10, 2635-2642. (In Chinese)
[11] Nabawy A. M., Samuel A. M., Samuel F. H., Doty, H. W., International Journal of Cast Metals Research. 26 (2013) 5, 308-317.
[12] Wang Xue-jiao, Xu Cong, Muhammad Arfan, Hanada Shuji, Yamagata Hiroshi, Wang Wen-hong, Ma Chao-li, Transactions of Nonferrous Metals Society of China. 24 (2014) 7, 2244-2250. (In Chinese)
[13] Mallapur D.G., Kori S.A., Udupa K. Rajendra, Journal of Materials Science. 46 (2011) 6, 1622-1627.
[14] Srirangam P., Chattopadhyay S., Bhattacharya A., Nag S., Kaduk J., Shankar S., Banerjee R., Shibata T., Acta Materialia. 65 (2014) 185-193.
[15] Cui X.L., Wu Y.Y., Gao T., Liu X.F., Journal of Alloys and Compounds. 615 (2014) 906-911.
[16] Tsai Y.C., Chou C.Y., Jeng R.R., Lee S.L., Lin C.K., International Journal of Cast Metals Research. 24 (2011) 2, 83-87.
[17] Chuanrong Qiu, Sainan Miao, Xinrong Li, Xingchuan Xia, Jian Ding, Yongning Wang, Weimin Zhao, Materials & Design. Article in press, available online 28 October 2016.
[18] Sui Yudong, Wang Qudong, Wang Guangliang, Liu Teng, Journal of Alloys and Compounds. 622 (2015) 572-579.